

Entanglement and transport through correlated quantum dot

Adam Rycerz

Instituut–Lorentz, Universiteit Leiden, P.O. Box 9506, NL–2300 RA Leiden, The Netherlands
 Marian Smoluchowski Institute of Physics, Jagiellonian University, Reymonta 4, 30-059 Kraków, Poland
 e-mail: adamr@th.if.uj.edu.pl

May 17, 2021

Abstract. We study quantum entanglement in a single–level quantum dot in the linear–response regime. The results show, that the maximal quantum value of the conductance $2e^2/h$ not always match the maximal entanglement. The pairwise entanglement between the quantum dot and the nearest atom of the lead is also analyzed by utilizing the Wootters formula for *charge* and *spin* degrees of freedom separately. The coexistence of zero concurrence and the maximal conductance is observed for low values of the dot–lead hybridization. Moreover, the pairwise concurrence vanish simultaneously for charge and spin degrees of freedom, when the Kondo resonance is present in the system. The values of a Kondo temperature, corresponding to the zero–concurrence boundary, are also provided.

PACS. 73.63.-b Electronic transport in nanoscale materials and structures – 03.65.Ud Entanglement and quantum nonlocality – 03.67.Mn Entanglement production, characterization, and manipulation

1 Introduction

Quantum entanglement, as one of the most intriguing features of quantum mechanics, was extensively studied during the last decade, mainly because its nonlocal connotation [1] is regarded as a valuable resource in quantum communication and information processing [2]. The question about the relation between the entanglement and quantum phase transitions [3] have been addressed recently, for either quantum spin [4, 5, 6, 7] and fermionic [8, 9, 10] systems, in hope to shed new lights on fundamental problems of condensed matter physics. For example, it was shown for spin model [4], that the entanglement of two neighboring sites displays a sharp peak either near or at critical point where quantum phase transition undergoes. Recently, a class of systems with divergent entanglement length away from quantum critical point, since the correlation length remains finite, was identified [5]. The spin–orbital entanglement analysis was also shown to provide a valuable insight to the nature of Mott insulators [6]. In the field of fermionic systems, the local entanglement was successfully used to identify quantum phase transitions in the extended Hubbard model [10]. A separate issue concerns using the entanglement as a criterion of quantum coherence [11] when analyzing nonequilibrium dynamics of the system with spontaneous symmetry breaking [7].

Here we follow the above ideas, but focus on the physical system which undergoes the crossover behavior instead of a phase transition: a quantum dot in the Kondo regime. *Namely*, we address the question *whether there exist a relation between entanglement and conductance* for this system? Some earlier study mentioned the total entanglement of electronic degrees of freedom in the $SU(4)$ system below the Kondo temperature, without determining a qualitative measure of such an entanglement [12]. In this paper, we consider the $SU(2)$ case, and

analyze two different definitions of the entanglement between quantum dot and the leads: *first* based on the von Neumann entropy, and *second* utilizing the Wootters formula [13] for the formation concurrence of two–qubit system.

2 The model and its numerical solutions

We study a model of a quantum dot with a single relevant electronic level coupled to the left (L) and right (R) metallic electrodes. The Hamiltonian of the system is

$$H = H_L + V_L + H_C + V_R + H_R; \quad (1)$$

where H_C models the central region, $H_{L(R)}$ describes the left (right) lead itself, and $V_{L(R)}$ is the coupling between the lead and the central region. Namely, we have

$$\begin{aligned}
 H_C &= \sum_d n_d + U n_d n_{d\#}; \\
 H_{L(R)} &= \sum_j t \sum_{j,j+1} c_j^\dagger c_{j+1} + h.c.; \\
 V_{L(R)} &= \sum_j V \sum_{j_L(R)} c_{j_L(R)}^\dagger d + h.c.;
 \end{aligned} \quad (2)$$

Here, $n_d = \sum_{\sigma} d^\dagger_{\sigma} d_{\sigma}$ is the quantum–dot charge, d_{σ} is the position of the molecular level and U is the Coulomb repulsion between two electrons. Both $H_{L(R)}$ and $V_{L(R)}$ terms have a tight–binding form, with the hopping t and the dot–lead hybridization parameter V , c_j^\dagger (c_j) creates (destroys) an electron with spin σ on site j , the indexes $j_{L(R)}$ denotes terminal sites of the left (right) electrode. The system is depicted schematically in Fig. 1.

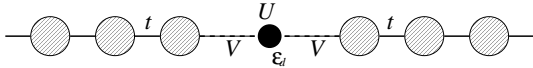


Fig. 1. The Anderson impurity model realized as a double quantum dot attached to the leads. The dot is described with the energy level ϵ_d and the Coulomb interaction U .

There are many theoretical methods in the existing literature, developed to study the electron transport in the presence of interaction. In particular, the zero-temperature conductance of the quantum dot acting as an Anderson impurity were obtained within the *Bethe ansatz* approach [14]. For the more general situation, one can refer to the *Numerical Renormalization Group* [15] or to the nonequilibrium *Keldysh formalism* [16]. For example, the former approach was successfully generalized to study a molecule with the electron-phonon coupling [17], whereas the latter was adapted for an analysis of the competition between the Fano and the Kondo resonance in various nanodevices [18].

However, since we are interested *either* in equilibrium transport properties *or* in the ground-state quantum entanglement, the most useful choice is the variational method recently proposed by Rejec and Ramšak [19,20], in which the real-space correlation functions are obtained directly. For the system described by the Hamiltonian (1) the method converges to the exact solution [14], it can also be generalized for multiple quantum dots [19], for the case with a nonzero magnetic field [20], or combined with an *ab initio* wave-function readjustment [21] in the framework of EDABI method [22].

3 The quantum entanglement

For the spin $s = 1/2$ fermionic system, there are four possible local states at each site, $|j, i_j\rangle = |j, i_j\rangle; |j, \bar{i}_j\rangle; |j, i_j\rangle; |j, \bar{i}_j\rangle$. The dimension of the N -site system is then 4^N and $|j_1; j_2; \dots; j_N\rangle = \prod_{j=1}^N |j, i_j\rangle$ are its natural basis vectors. Alternatively, one can label the basis vectors by specifying occupation numbers for each site and spin $|j_1; j_2; \dots; j_N\rangle = |n_{1\uparrow}; n_{1\downarrow}; n_{2\uparrow}; n_{2\downarrow}; \dots; n_{N\uparrow}; n_{N\downarrow}\rangle$; with $n_j = 0; 1$. The reduced density matrix for the ground state $|j\rangle$ is

$$\rho_{i,j} = \text{Tr}_{i',j'} \rho_{i',j'} \quad (3)$$

where $\text{Tr}_{i',j'}$ stands for tracing over all sites and spins except the i and j -th sites.

3.1 Local entanglement and conductance

We focus now on the local entanglement [9], which exhibits the quantum correlations between local state of a selected j -th site (e.g. the quantum dot) and the other part of the system (here: the leads). For $i = j = d$ and $\rho_{i,j}$, the reduced density matrix, defined by Eq. (3), takes the form

$$\rho_{i,j} = u_+ |j, i\rangle\langle j, i| + w_1 |j, \bar{i}\rangle\langle j, \bar{i}| + w_2 |j, i\rangle\langle j, \bar{i}| + u_- |j, \bar{i}\rangle\langle j, i| \quad (4)$$

where

$$u_{\pm} = \frac{1}{2} (1 \pm \frac{2V}{U}) \quad w_{\pm} = \frac{1}{2} (1 \mp \frac{2V}{U})$$

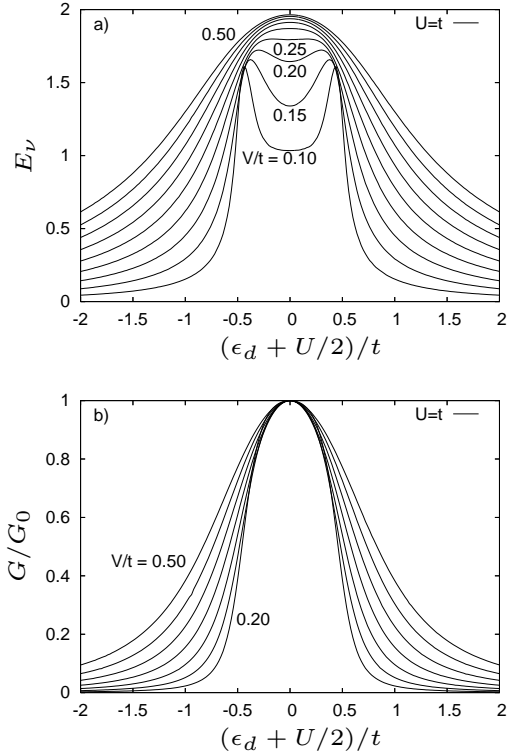


Fig. 2. The local entanglement (a) and normalized conductance (b) for the system in Fig. 1 as a function of the dot energy level ϵ_d and dot-lead hybridization V (changed in steps of $0.05t$).

$$w_{\pm} = \frac{1}{2} (1 \mp \frac{2V}{U}) \quad u_{\pm} = \frac{1}{2} (1 \pm \frac{2V}{U}) \quad (5)$$

and the averaging is performed for the system ground state. Consequently, the corresponding von Neumann entropy E_v (hereinafter called the *local entanglement*) measures the entanglement of the states of quantum dot ($j = d$) with that of the remaining $N - 1$ sites, and is given by

$$E_v = -u_+ \log_2 u_+ - w_1 \log_2 w_1 - w_2 \log_2 w_2 - u_- \log_2 u_- \quad (6)$$

In Fig. 2 we compare the the local entanglement E_v with the conductance calculated from the Rejec-Ramšak *two-point formula* [19]

$$G = G_0 \sin^2 \frac{E(\epsilon_F) - E(0)}{2} \quad (7)$$

where $G_0 = 2e^2/h$ is the conductance quantum, $\epsilon_F = 1/N \sum_{i=1}^N \epsilon_i$ is the average level spacing at Fermi energy, determined by the density of states in an infinite lead $\rho(\epsilon_F)$, $E(\epsilon_F)$ and $E(0)$ are the ground-state energies of the system with *periodic* and *antiperiodic* boundary conditions, respectively. We found that the system size of the order of $N = 1000$ provides an excellent convergence for both the conductance G and the local entanglement E_v (the latter aspect has not been analyzed numerically before). In particular, the data for $N = 1000$ cannot be distinguished from the ones for $N = 2000$ in the scale of Fig. 2. We also checked that the results are insensitive to the number of basis functions composing the Rejec-Ramšak vari-

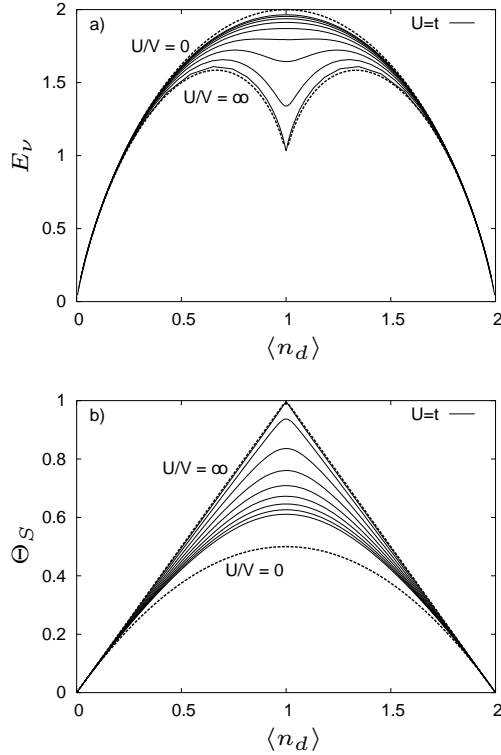


Fig. 3. The local entanglement E_v (a) and spin-magnitude parameter Θ_S (b) as a function of the dot filling $\langle n_d \rangle$ and dot-lead hybridization V . The magnitude of hybridization V goes from $0.1t$ to $0.5t$ in steps of $0.05t$. The limiting curves for $U=V = 0$ and $U=V = 1$ are depicted with *dashed* lines.

ational wave-function [19], providing it is > 3 . When calculating correlation functions (5), determining the density matrix (4), one has to choose boundary conditions which minimize the ground-state energy for a given system size N : namely, periodic for $N = 4k + 2$, and antiperiodic for $N = 4k$ [23] for the half-filling [24].

Surprisingly, the maximal entanglement between a quantum dot and leads not always match the maximal conductance $G = G_0 = 2e^2/h$. For small values of the dot-lead hybridization ($V \ll 0.25t$ for $U = t$), E_v has a minimum at the particle-hole symmetric point $\langle n_d \rangle = U=2$. It is well known [25] that in the limit $V \ll t \ll U$ the Anderson Hamiltonian (1) reduces to the symmetric Kondo model with an exchange coupling $(J_K)_{\text{eff}} = 8V^2 = U \frac{t^2}{4t^2 - U^2}$. This observation suggests an important role of the localized moment presence in the dot, which strongly affects the entanglement between the quantum dot and the leads, without observable change to the conductance. The latter refers to the situation below the Kondo temperature $T_K \sim \exp(-1/(J_K))$, above which the conductance at the particle-hole symmetric point $\langle n_d \rangle = U=2$ is depressed and, subsequently, each zero-T Kondo peak displayed on Fig. 2b splits into Coulomb-blockade peaks present in a finite-T situation [15, 16, 17, 18]. In particular, for $U = t$ and $V = 0.25t$, the exact formula [26] gives the value of $T_K = t \frac{3m_K}{eV}$, which seems to be in the experimentally accessible range. A finite-T analysis is, however, beyond the

scope of this paper, since we focus here on $T = 0$ situation. A further discussion of the relation between spin fluctuations and the entanglement at the ground state is provided below.

For the better overview of the system properties we analyze them as functions of the dot filling $\langle n_d \rangle$, as displayed in Fig. 3. The universal formula for the conductance (not shown) follows from the Luttinger theorem [27]

$$G = G_0 \sin^2(\langle n_d \rangle); \quad (8)$$

whereas E_v evolves gradually from the limit

$$E_v^{U=0} = \langle n_d \rangle \log_2 \frac{\langle n_d \rangle}{2} - (2 - \langle n_d \rangle) \log_2 (1 - \frac{\langle n_d \rangle}{2}) \quad (9)$$

to

$$E_v^{U=1} = (1 - \langle n_d \rangle) \log_2 (1 - \langle n_d \rangle) + \langle n_d \rangle \log_2 \frac{\langle n_d \rangle}{2}; \quad (10)$$

as presented in Fig. 3a. Therefore, in the strong coupling limit E_v has two maxima at $\langle n_d \rangle = 2=3$ and $4=3$, instead of a single one for $\langle n_d \rangle = 1$, present in the noninteracting case. The major qualitative difference between our results and that obtained for the extended Hubbard model [10] is that E_v behaves analytically for any $U < 1$. This is because the Kondo system, considered here, shows the crossover behavior instead of a quantum phase transition present in the Hubbard chain.

One can also observe, that the entanglement behavior near the particle-hole symmetric point $\langle n_d \rangle = 1$ is determined by the magnitude of spin fluctuations, presented in Fig. 3b. As a measure of such fluctuations, we choose a parameter [28]

$$s = \frac{4}{3} \langle n_d \rangle^2 = \langle n_d \rangle - 2 \langle n_d \rangle^2; \quad (11)$$

which obeys the inequality

$$\langle n_d \rangle - 1 \leq \frac{\langle n_d \rangle}{2} \leq s \leq 1 - \langle n_d \rangle; \quad (12)$$

where the lower and the upper limit refers to the $U = 0$ and $U = 1$ case, respectively. In particular, for $\langle n_d \rangle = 1$ the spin-fluctuation parameter varies from $s = 1=2$ for free fermions to $s = 1$ for the localized spin-1=2. The charge fluctuations are determined by s as $\text{Var}(\langle n_d \rangle) = \langle n_d \rangle^2 = \langle n_d \rangle(2 - \langle n_d \rangle) - s$, so for $\langle n_d \rangle = 1$ and $U = 1$ we obtain $\text{Var}(\langle n_d \rangle) = 0$. The vanishing of charge fluctuations and the value of the spin-square $s = 3=4$ allows one to consider the localized spin 1=2, a presence of which governs the ground-state properties at the strong-coupling limit. The density matrix (4) takes thus the form $\rho = (|1\rangle\langle 1| + |2\rangle\langle 2|)/2$, which brought us to the value of the local entanglement $E_v = 1$ at the particle-hole symmetric point. In contrast, for the noninteracting system all coefficients of the density matrix (4) are equal to $1=4$ and the local entanglement reaches its maximal value $E_v = 2$ (for $\langle n_d \rangle = 1$). The entanglement drop with the increasing coupling near the particle-hole symmetric point can therefore be explained as an effect of the formation of a localized moment inside the dot.

The correspondence between inequalities (12) and the limits defined by Eqs. (9) and (10) become straightforward when

expressing the coefficients of the density matrix (4) as functions of n_{di} and s , what leads to the local entanglement

$$E_v = \frac{2}{2} \frac{n_{di}}{2} s \log_2 \frac{2}{2} \frac{n_{di}}{2} s \log_2 \frac{s}{2} : (13)$$

Eq. (13) with the limits given by (12) relates the entanglement between the quantum dot and the leads to the local moment formation inside the dot. It also expresses the local entanglement E_v in terms of measurable quantities: the dot occupation n_{di} and the spin-square magnitude s^2 contained in the parameter s (11). In contrast, the spin fluctuations are absent in Eq. (8) for the conductance G , which is fully determined by the dot filling n_{di} . One can note Eq. (13) is model-independent, providing we consider the lattice system with one orbital per site. Thus, for the system with quantum phase transition, such as that considered by Gu *et al.* [10], the nonanalytical behavior of the local entanglement E_v is equivalent to the nonanalytical behavior of the spin-magnitude parameter s .

3.2 The fermionic concurrence

We consider here the entanglement of two qubits, one associated with the electron localized on a quantum dot and other with the nearest one placed in a lead. The physical realization of individual qubits may, in principle, employ *charge* or *spin* degrees of freedom of the system in Fig. 1.

The reduced density matrix (3) for the pair of electrons with equal spins (say \uparrow), one localized on a quantum dot and other on a nearest lead atom ($i = d, j = j_L(R)$), can be written as [29]

$$\rho_{i,j}^c = \begin{pmatrix} 0 & u_+^c & 0 & 0 & 0 & 1 \\ 0 & w_1^c & z^c & 0 & 0 & 0 \\ 0 & (z^c)^* & w_2^c & 0 & 0 & 0 \\ 0 & 0 & 0 & u^-^c & 0 & 0 \end{pmatrix} ; \quad (14)$$

where

$$u_+^c = h(1 - n_{i\#})(1 - n_{j\#})i; \quad w_1^c = h n_{i\#}(1 - n_{j\#})i; \\ w_2^c = h(1 - n_{i\#})n_{j\#}i; \quad z^c = h c_{j\#}^y c_{i\#}^y i; \quad u^-^c = h n_{i\#} n_{j\#} i; \quad (15)$$

The upper index c stands to denote, that the density matrix (14) refers to the *charge* degrees of freedom, since the *spin* direction is arbitrarily chosen for both particles.

We use now the *concurrence* C as a measure of the entanglement for such a two-qubit system. The closed-form expression, derived by Wootters [13], reads

$$C = \max \left\{ 0, \sqrt{\frac{p_1 - p_2}{2}}, \sqrt{\frac{p_2 - p_3}{2}}, \sqrt{\frac{p_3 - p_4}{2}} \right\} : \quad (16)$$

The p_i 's are the eigenvalues of the matrix product $\begin{pmatrix} \tilde{y} & \tilde{y} \\ \tilde{y} & \tilde{y} \end{pmatrix} \begin{pmatrix} \tilde{y} & \tilde{y} \\ \tilde{y} & \tilde{y} \end{pmatrix}$, and $p_1 > p_2 > p_3 > p_4$. Since there exists a monotonous relation between the concurrence C and the entanglement of formation $E_f = -x \log_2 x - (1-x) \log_2 (1-x)$,

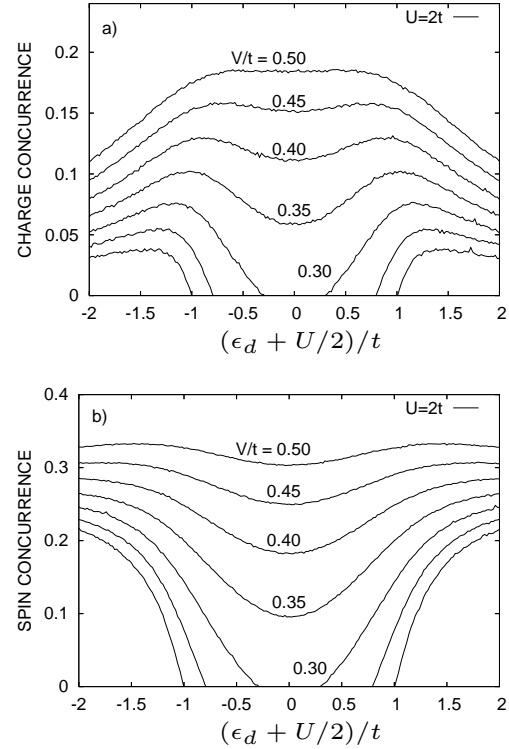


Fig. 4. The charge (a) and spin (b) pairwise concurrence for the system containing one qubit localized on quantum dot and other on the nearest atom of the lead.

where $x = \frac{1}{2} \pm \sqrt{\frac{1}{2} (C^2 - 2)}$ [13], C is widely used instead of E_f in the literature.

For the density matrix $\rho_{i,j}^c$ (14) the corresponding concurrence can be calculated from Eq. (16) as

$$C_{i,j}^c = \max \left\{ 0, \sqrt{\frac{p_1 - p_2}{2}}, \sqrt{\frac{p_2 - p_3}{2}}, \sqrt{\frac{p_3 - p_4}{2}} \right\} : \quad (17)$$

Hereinafter, we call $C_{i,j}^c$ a *charge concurrence*, since it is related to the charge degrees of freedom.

Alternatively, one can consider the full two-site density matrix $\rho_{ij}^s = \text{Tr}_{i,j} \rho_{ij}^s$ (with $i = d$, and $j = j_L(R)$ again) and project out all the states except from these corresponding to $n_i = n_j = 1$. The resultant 4×4 density matrix $\tilde{\rho}_{s_i, s_j}^s = \text{Tr}_{\sim s_i, s_j} \rho_{ij}^s$ describes the entanglement accessible by spin manipulation with a particle-conservation constrain [30]. The matrix $\tilde{\rho}_{s_i, s_j}^s$ has a general structure of $\rho_{i,j}^c$ given by Eq. (14), with the elements (15) replaced by

$$u_+^s = h n_{i\#}(1 - n_{j\#})i; \quad w_1^s = h(1 - n_{i\#})n_{j\#}i; \\ w_2^s = h(1 - n_{i\#})n_{j\#}i; \quad z^s = h c_{j\#}^y c_{i\#}^y i; \\ u^-^s = h n_{i\#} n_{j\#} i; \quad (18)$$

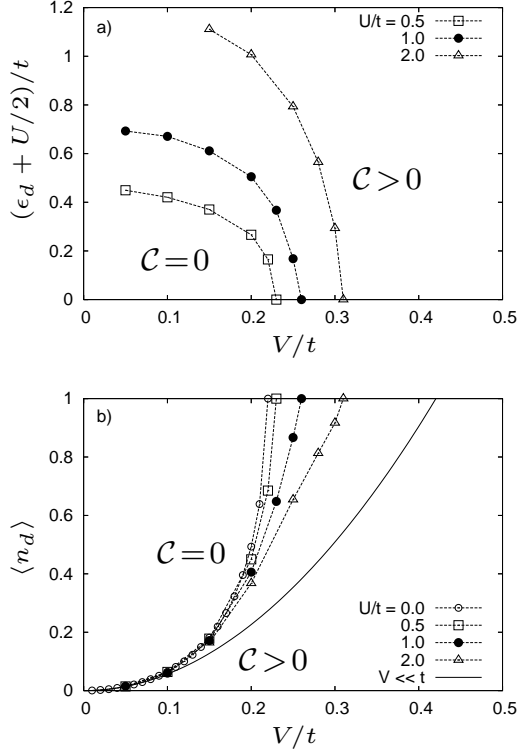


Fig. 5. The values of dot energy level ϵ_d (a) and average occupation $\langle n_d \rangle$ (b) corresponding to zero concurrence, as a function of hybridization V and Coulomb interaction U (specified for each dataset). The perturbative limit $V \leq t$ is also shown.

The labels indicate that we are working now with the *spin* degrees of freedom, as charges of the i and j sites are chosen. The concurrence, obtained by applying the definition (16) to the density matrix $\rho_{s_i s_j}$, is called a *spin concurrence*.

The charge and spin concurrence is shown in Fig. 4 as a function of the dot energy level ϵ_d . Again, we observe an excellent convergence of both the studied quantities for the system size of the order of $N = 1000$. Although the charge and spin concurrence are, in principle, two different physical quantities, they reach the limit $C = 0$ simultaneously for all the analyzed values of V and U . Therefore, we can conclude that below the critical value of the hybridization $V < V_c(U)$ and in the Kondo regime, the qubit localized on the quantum dot is not entangled with other placed on the top of the lead for *neither charge nor spin* degrees of freedom. This is because of large quantum fluctuations in each lead (modeled as a noninteracting Fermi gas), which therefore destroy the entanglement for a weak dot-lead coupling.

The values of ϵ_d and $\langle n_d \rangle$, corresponding to $C = 0$ are depicted in Fig. 5. To complement the analysis we also provide, in Table 1, the values of the symmetric Kondo temperature [26], corresponding to the critical hybridization $V_c(U)$, at which the concurrence vanishes in the ground state. Although the numerical results presented in Fig. 5 refer to $T = 0$, it is clear that in the finite- T situation the conductance $G = G_0$ at the particle-hole symmetric point if $T = T_K$, and that the concurrence C decreases with T due to dephasing. Therefore we can conclude,

Table 1. The critical values of hybridization V_c on the zero-concurrence boundary for $\epsilon_d = U/2$, the corresponding exchange coupling $(0)J_K = 4V^2 = U t$, and the Kondo temperature [26].

$U=t$	V_c	$(0)J_K$	$T_K = t$ [mK = eV]
0.5	0.23	0.135	360
1.0	0.26	0.086	8.6
2.0	0.31	0.061	0.13

that the coexistence of zero concurrence and maximal conductance can be observed for $U \leq t$ if the relative temperature $T=t$ is of the order of a few mK = eV. Another interesting feature of these results is the universal (interaction independent) behavior of the maximal dot filling $\langle n_d \rangle = \langle n_d \rangle_{\max}$, for which the entanglement $C > 0$, with $V=t \rightarrow 0$ (cf. Fig. 5b). This observation can be rationalized by using Eq. (17) and putting $C_{i^n; j^n} = 0$. Then, in the perturbative limit $V \leq t$, we obtain

$$\langle n_d \rangle_{\max} = 2^{3=2} \sum_{i,j} c_i^\dagger c_j = 2^{5=2} (V=t)^2;$$

up to the quadratic terms. The agreement with the numerical data is perfect for $V=t \leq 0.1$.

4 Summary

We analyzed the local entanglement between the quantum dot and the leads as a function of the dot energy level ϵ_d , the dot-lead hybridization V and the intra-dot Coulomb repulsion U . The measure of this entanglement, the von Neumann entropy E_v , evolves gradually from the *weak-coupling* limit, in which the maximal E_v match the maximal quantum value of the conductance $G = G_0 = 2e^2/h$, to the *strong-coupling* situation, where maximal G corresponds to the local minimum of E_v . This behavior was explained in terms of local moment formation inside the dot, which took place when the charge transport is dominated by the Kondo effect.

Finally, we defined the pairwise concurrence, measuring the entanglement between a pair of qubits: one localized on the dot and other on the nearest atom of the lead, for *charge* and *spin* degrees of freedom separately. Both quantities vanish simultaneously in the Kondo-resonance range, where the weakly-entangled system shows the maximal conductance. We predict the latter to be observable at the temperature range of $T=W \sim 1$ mK = eV (where $W = 4t$ is the lead bandwidth), which seems to be accessible within the present nanoscale experimental techniques. The universal dependence of the maximal dot filling, above which the concurrence vanishes, $\langle n_d \rangle_{\max} = 2^{5=2} (V=t)^2$ for $V=t \leq 1$, was also identified.

Acknowledgment

I am grateful to Prof. C. W. J. Beenakker for many discussions and comments. Remarks by Profs. M. A. Martin-Delgado, A.

M. Oleś, J. Spałek, and Drs. B. Trauzettel, D. Sanchez are appreciated. The work was supported by the Polish Science Foundation (FNP) Foreign Postdoc Fellowship, and by Polish Ministry of Education and Science, Grant No. 1 P03B 001 29.

References

1. A. Einstein, B. Podolski, and N. Rosen, *Phys. Rev.* **47**, 777 (1935).
2. See review by C. H. Bennet and D. P. Divincenzo, *Nature* **404**, 247 (2000); M. A. Nielsen and I. L. Chuang, *Quantum Computation and Quantum Information* (Cambridge, 2000).
3. S. Sachdev, *Quantum Phase Transitions* (Cambridge University Press, Cambridge, 2000).
4. A. Osterloh *et al.*, *Nature* **416**, 608 (2002); T. J. Osborne and M. A. Nielsen, *Phys. Rev. A* **66**, 032110 (2002); V. Subrahmanyam, *ibid.* **69**, 022311 (2004).
5. F. Verstraete, M. A. Martin-Delgado, J. I. Cirac, *Phys. Rev. Lett.* **92**, 087201 (2004); M. Popp *et al.*, quant-ph/0411123, unpublished.
6. A. M. Oleś *et al.*, *Phys. Rev. Lett.* **96**, 147205 (2006).
7. J. van Wezel, J. van den Brink, J. Zaanen, *Phys. Rev. Lett.* **94**, 230401 (2005).
8. J. Schliemann, D. Loss, A. H. MacDonald, *Phys. Rev. B* **63**, 085311 (2001); J. Schliemann *et al.*, *Phys. Rev. A* **64**, 022303 (2001).
9. P. Zanardi, *Phys. Rev. A* **65**, 042101 (2002); P. Zanardi, X. Wang, *J. Phys. A* **35**, 7947 (2002).
10. S.-J. Gu *et al.*, *Phys. Rev. Lett.* **93**, 086402 (2004).
11. A. O. Caldeira and A. J. Leggett, *Phys. Rev. Lett.* **46**, 211 (1981); I. L. Chuang *et al.*, *Science* **270**, 1633 (1995).
12. M.-S. Choi, R. López, R. Aguado, *Phys. Rev. Lett.* **95**, 067204 (2005); R. López *et al.*, *Phys. Rev. B* **71**, 115312 (2005).
13. W. K. Wootters, *Phys. Rev. Lett.* **80**, 2245 (1998); S. Hill, W. K. Wootters, *Phys. Rev. Lett.* **78**, 5022 (1997).
14. P. B. Wiegman, A. M. Tsvelick, *Pis'ma ZETF* **35**, 100 (1982); *J. Phys. C* **16**, 2281 (1983).
15. W. Hofstetter, J. König, and H. Schoeller, *Phys. Rev. Lett.* **87**, 156803 (2001).
16. Y. Meir, N. S. Wingreen, *Phys. Rev. Lett.* **68**, 2512 (1992); A.-P. Jauho *et al.*, *Phys. Rev. B* **50**, 5528 (1994).
17. P. S. Cornaglia *et al.*, *Phys. Rev. Lett.* **93**, 147201 (2004).
18. P. Stefański, A. Tagliacozzo, B. Bułka, *Phys. Rev. Lett.* **93**, 186805 (2004); B. Bułka, P. Stefański, *ibid.* **86**, 5128 (2001).
19. T. Rejec, A. Ramšak, *Phys. Rev. B* **68**, 035342 (2003).
20. T. Rejec, A. Ramšak, *Phys. Rev. B* **68**, 033306 (2003).
21. A. Rycerz, J. Spałek, cond-mat/0604237, to be published.
22. A. Rycerz, J. Spałek, *Eur. Phys. J. B* **40**, 153 (2004); *Phys. Rev. B* **63**, 073101 (2001); *ibid.* **65**, 035110 (2002).
23. E. H. Lieb, *Phys. Rev. Lett.* **73**, 2158 (1994); F. Nakano, *J. Phys. A* **33**, 5429 (2000); *ibid.* **37**, 3979 (2004). For a discussion of boundary condition role in even/odd effect for correlated nanosystems see: A. Rycerz, J. Spałek, *phys. stat. sol. (b)* **243**, 183 (2006).
24. The notion of the half-filling refers to the entire system composed of a quantum dot and leads, as presented in Fig. 1. The average dot occupation $\langle n_d \rangle$ is determined by the energy level ϵ_d , and reaches 1 at the particle-hole symmetric point $\epsilon_d = U=2$.
25. J. Kondo, *Prog. Theor. Phys.* **28**, 846 (1962); J. R. Schrieffer, P. A. Wolf, *Phys. Rev.* **149**, 491 (1966).
26. The symmetric Kondo temperature for $\epsilon_d = U=2$ [14] is given by $T_K = \frac{p}{2U} \exp\left(\frac{U=8}{(V_F)^2} \right)$, with the impurity level width $\Gamma = \frac{p}{V^2} = \frac{p}{4t^2 V_F}$, where the second equality refers to the tight-binding electrodes shown in Fig. 1.
27. A. C. Hewson, *The Kondo Problem to Heavy Fermions* (Cambridge University Press, 1997).
28. J. Spałek, *J. Sol. St. Chem.* **88**, 70 (1990); J. Spałek, A. M. Oleś, J. M. Honig, *Phys. Rev. B* **28**, 6802 (1983).
29. For an application to the Hubbard dimer, see: S.-S. Deng, S.-J. Gu, H.-Q. Lin, *Chin. Phys. Lett.* **22**, 804 (2005). The generalization for any two neighboring sites of one-dimensional system with one orbital per site is straightforward.
30. See, e.g. C. W. J. Beenakker, cond-mat/0508488, to be published in *Quantum Computers, Algorithms and Chaos*, Int. School of Phys. "Enrico Fermi", vol. 162, and references therein.